The iron–siderophore transporter FhuA is the receptor for the antimicrobial peptide microcin J25: role of the microcin Val[11]–Pro[16] β-hairpin region in the recognition mechanism

Delphine DESTOUMIEUX-GARZÓN*[1], Sophie DUQUESNE*, Jean PEDUZZI*, Christophe GOULARD*, Michel DESMADRIL†, Lucienne LETELLIER†, Sylvie REBUFFAT* and Pascale BOULANGER†

*Chimie et Biochimie des Substances Naturelles, CNRS UMR 5154, Muséum National d'Histoire Naturelle USM 502, Département Régulations Développement et Diversité Moléculaire, 63 rue Buffon, 75005 Paris, France, and †Institut de Biochimie et Biophysique Moléculaire et Cellulaire, CNRS UMR 8619, Université de Paris-Sud, 91405 Orsay cedex, France

The role of the outer-membrane iron transporter FhuA as a potential receptor for the antimicrobial peptide MccJ25 (microcin J25) was studied through a series of *in vivo* and *in vitro* experiments. The requirement for both FhuA and the inner-membrane TonB–ExbB–ExbD complex was demonstrated by antibacterial assays using complementation of an *fhuA*$^-$ strain and by using isogenic strains mutated in genes encoding the protein complex respectively. In addition, MccJ25 was shown to block phage T5 infection of *Escherichia coli*, *in vivo*, by inhibiting phage adhesion, which suggested that MccJ25 prevents the interaction between the phage and its receptor FhuA. This *in vivo* activity was confirmed *in vitro*, as MccJ25 inhibited phage T5 DNA ejection triggered by purified FhuA. Direct interaction of MccJ25 with FhuA was demonstrated for the first time by size-exclusion chromatography and isothermal titration calorimetry. MccJ25 bound to FhuA with a 2:1 stoichiometry and a K_d of 1.2 μM. Taken together, our results demonstrate that FhuA is the receptor for MccJ25 and that the ligand–receptor interaction may occur in the absence of other components of the bacterial membrane. Finally, both differential scanning calorimetry and antimicrobial assays showed that MccJ25 binding involves external loops of FhuA. Unlike native MccJ25, a thermolysin-cleaved MccJ25 variant was unable to bind to FhuA and failed to prevent phage T5 infection of *E. coli*. Therefore the Val[11]–Pro[16] β-hairpin region of MccJ25, which is disrupted upon cleavage by thermolysin, is required for microcin recognition.

Key words: antimicrobial peptide, FhuA, iron transporter, microcalorimetry, microcin, phage T5.

INTRODUCTION

Microcins are gene-encoded antimicrobial (poly)peptides secreted by Enterobacteriaceae. Produced under conditions of nutrient depletion, they are active against phylogenetically related microbial strains. Therefore they are considered to play a major role in the regulation of microbial competition within the intestinal flora. MccJ25 (microcin J25) is naturally secreted by the faecal *Escherichia coli* AY25 strain [1]. The 21-residue mature MccJ25 (2.1 kDa) was isolated from culture supernatants [2]. It exhibits a side-chain-to-backbone cyclization involving Glu[8] and the N-terminal glycine, and adopts a lasso-structure in which the C-terminal end of the peptide is threaded into the cyclic backbone [3]. We have shown recently that the two-chain analogue t-MccJ25 (initially called MccJ25-L [2]), obtained by cleavage with thermolysin, retains the lasso-structure of MccJ25 but loses the Val[11]–Pro[16] hairpin-like structure targeted by the enzyme [4] (Figure 1). Interestingly, the highly potent activity of MccJ25 decreases markedly, but is not fully abrogated, upon thermolysin cleavage [5], indicating that the targeted region is required for complete antibacterial activity.

Major progress has been made in characterizing the mechanism of action of MccJ25 in *E. coli*. Indeed, MccJ25 was shown to inhibit transcription by targeting the β' subunit of RNA polymerase [6,7]. The molecular mechanism involves MccJ25 binding and obstruction of the RNA polymerase secondary channel, which in turn prevents the correct positioning of NTP substrates [8,9]. Conversely, few studies have addressed MccJ25 recognition at bacterial membranes. Previous studies have shown that MccJ25-resistant bacteria displayed mutations in the *fhuA*, *tonB* or *sbmA* gene, indicating that the outer-membrane protein FhuA, as well as the inner-membrane proteins TonB and SbmA, are likely to be involved in MccJ25 uptake [10,11].

The *E. coli* outer-membrane protein FhuA (79 kDa) is a high-affinity transporter for iron chelated to the siderophore ferrichrome (for a review, see [12]). FhuA is a multifunctional protein. Indeed, besides its physiological function, FhuA also transports the antibiotics albomycin and rifamycin CGP4832, and serves as a receptor for the bacterial toxin colicin M and for the unrelated phages T1, T5 and Φ80 [13]. Iron–ferrichrome transport across the outer membrane, as well as irreversible binding of phages T1 and Φ80 to the outer membrane, requires an energized cytoplasmic membrane. These functions of FhuA are coupled to the electrochemical gradient of protons via the cytoplasmic membrane-anchored TonB–ExbB–ExbD complex [12,14]. The three-dimensional structure of FhuA reveals a 22-stranded antiparallel β-barrel with an N-terminal globular domain folded inside the barrel. This plug domain spans most of the interior of the barrel and occludes it. The four-stranded β-sheet and the four short helices forming the plug are connected to the β-barrel and to the

Abbreviations used: c.f.u., colony-forming units; DSC, differential scanning calorimetry; ITC, isothermal titration calorimetry; LB, Luria–Bertani; MBC, minimum bactericidal concentration; MccJ25, microcin J25; t-MccJ25, two-chain analogue obtained by cleavage of MccJ25 with thermolysin; MIC, mimimum inhibitory concentration; MOI, multiplicity of infection; p.f.u., plaque-forming units; TFA, trifluoroacetic acid; YO-PRO-1, quinolinium {4-[(3-methyl-2(3H)-benzoxazolylidene)methyl]-1-[3-(trimethylammonio)propyl]}.

[1] To whom correspondence should be addressed (email ddestoum@mnhn.fr).

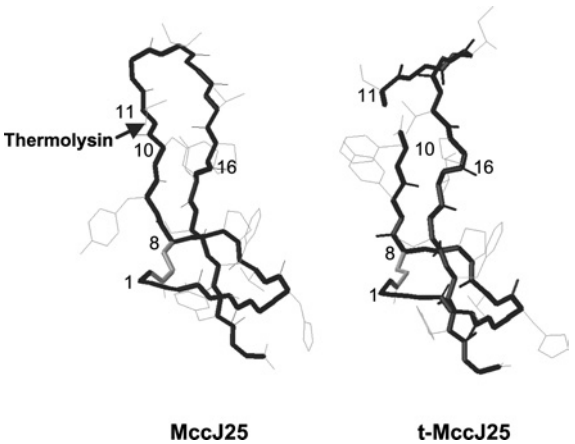

Figure 1 Structural comparison of native MccJ25 (PDB entry 1Q71) and thermolysin-cleaved t-MccJ25 (PDB entry 1S7P)

The Figure illustrates the disruption of the MccJ25 Val^{10}–Pro^{16} β-hairpin upon cleavage by thermolysin. Structures are represented with black backbones and grey side chains using MOLMOL software [38]. Thick covalent bonds were used for the peptide backbones as well as the Glu^{8} side chain engaged in the ring. The Val^{10}–Phe^{11} bond targeted by thermolysin is indicated by an arrow. Selected residues are numbered.

external hydrophilic loops by numerous hydrogen bonds and salt bridges [15]. The binding sites for the different FhuA ligands are located on the external loops of the barrel [16].

The involvement of FhuA in susceptibility to MccJ25 was supported by the observation that a FhuA-deficient *E. coli* strain resistant to MccJ25 was rendered susceptible upon transfection with a plasmid encoding the *E. coli* or *Salmonella enteritidis* Paratyphi FhuA protein, but not when plasmids encoding *S. enteritidis* Typhimurium or *Pantoea agglomerans* (previously *Erwinia herbicola*) FhuA were used [17]. Similarly, when *S. enteritidis* Typhimurium, which is resistant to MccJ25, was transfected with a plasmid encoding the *E. coli* FhuA protein, it became highly susceptible to the microcin [18]. These data strongly suggest that FhuA behaves as a receptor for MccJ25, and that strain susceptibility could vary according to the affinity between MccJ25 and the FhuA protein.

Despite such indirect evidence for a role for FhuA in MccJ25 recognition, previous studies have paid little or no attention to the molecular basis of the recognition mechanism. In the present paper, we have studied the role of FhuA as a receptor for MccJ25, with regard to (i) the conditions for potential MccJ25–FhuA complex formation, (ii) the nature of the regions of MccJ25 and FhuA involved, and (iii) the effect of MccJ25 binding on FhuA-dependent functions. *In vivo*, MccJ25 was used to inhibit FhuA-mediated functions such as phage T5-induced bacterial lysis. *In vitro*, the MccJ25–FhuA molecular interaction was studied and the affinity constant of MccJ25 for FhuA was measured. Finally, the role of the Val^{11}–Pro^{16} β-hairpin region of MccJ25 in the microcin recognition step was evaluated by comparing the inhibitory activity of MccJ25 on FhuA-dependent functions with that of the thermolysin-cleaved t-MccJ25, as well as the affinities of MccJ25 and t-MccJ25 for the FhuA protein.

EXPERIMENTAL

Micro-organisms

Bacterial strains used for MccJ25 and FhuA expression were *E. coli* MC4100 carrying the pTUC202 plasmid [19] (a gift from Professor Felipe Moreno, Hospital Ramón y Cajal, Madrid, Spain) and *E. coli* HO830*fhuA* carrying the pHX405 plasmid [20] respectively. Bioassays were performed with the bacterial strains described previously [21,22], as well as with *S. enterica* Paratyphi SL369 [23], *S. enterica* Typhimurium LT2 [23], *P. agglomerans* K4 [24] (generously provided by Professor Volkmar Braun, University of Tübingen, Germany) and *Pseudomonas aeruginosa* A.T.C.C. 27853 (a gift from Professor Alain Reynaud, Hospital of Nantes, France). Studies on the inhibition of viral adsorption and/or lysis were performed with *E. coli* strains susceptible to phage T5 infection, namely *E. coli* W3110 [25] and *E. coli* F, a fast-adsorbing strain of phage T5 [26]. Stocks of phage T5 [1×10^{12} p.f.u. (plaque-forming units)/ml] were prepared according to [27].

Peptide and protein purification

MccJ25 and FhuA were purified as described previously [2,28] and quantified by amino acid composition analysis as in [21] (MccJ25), or by using the ε_M (103 690 $M^{-1} \cdot cm^{-1}$) deduced from amino acid content (FhuA). Production of ^{3}H-radiolabelled MccJ25 was achieved by growing *E. coli* MC4100 pTUC202 in M63 medium supplemented with a mixture of amino acids (50 μM each) without glycine, containing 1 mg/l thiamine, 0.02 % (w/v) $MgSO_4$, 0.02 % (w/v) glucose, 30 μg/ml chloramphenicol and 0.46 MBq of [^{3}H]glycine (592 GBq/mmol; Amersham Biosciences). After a 16 h incubation at 37 °C, the culture supernatant was subjected to solid-phase extraction on a SepPak C_{18} cartridge (Waters Corp.) pre-equilibrated with 0.1 % (v/v) aqueous TFA (trifluoroacetic acid). After a washing step in 0.1 % TFA, successive elution steps were performed at 25 and 30 % (v/v) acetonitrile in 0.1 % TFA. The 30 % (v/v) acetonitrile fraction containing [^{3}H]MccJ25 was concentrated under vacuum in a SpeedVac concentrator (Savant) and loaded on to a C_{18} μBondapak column (10 μm, 300 mm × 3.9 mm; Waters Corp.) for final purification. Elution was performed with a linear gradient of 0–60 % (v/v) acetonitrile in 0.1 % (v/v) TFA over 30 min at a flow rate of 1 ml/min. Absorbance was monitored at 226 nm and fractions were collected manually. The specific radioactivity of [^{3}H]MccJ25 was determined by radioactivity counting (Pharmacia Wallac 1410 liquid-scintillation counter), and peptide quantification was performed by amino acid composition analysis as described previously [29]. Peptide antibacterial activity was finally controlled according to the protocol described below.

Antibacterial assays

Peptide antibacterial activity was assayed using the liquid growth inhibition assay described previously [21]. Briefly, serial dilutions of MccJ25 or t-MccJ25 (10 μl) were incubated in a 96-well microtitre plate with 90 μl of a mid-exponential phase culture of bacteria at a starting attenuance of 0.001 at 620 nm in Poor-Broth nutrient medium (1 % bactotryptone and 0.5 % NaCl). Bacterial growth was monitored by attenuance measurement at 620 nm in a Ceres 900 (Bio-Tek Instruments) plate recorder after a 20 h incubation at 30 °C. Samples of 100 μl from wells displaying no apparent growth were plated on LB (Luria–Bertani) agar plates and incubated for 16 h at 37 °C in order to detect potential bactericidal effects. The MIC (minimum inhibitory concentration) and MBC (minimum bactericidal concentration) values are expressed as the lowest concentration (μM) that caused 100 % inhibition of growth in liquid medium or on agar plates respectively.

Inhibition of infection with phage T5

A suspension of *E. coli* W3110 at 5×10^8 c.f.u. (colony-forming units)/ml was prepared in fresh LB medium from a culture in the exponential phase of growth. An aliquot of 100 μl of the bacterial

suspension was then incubated for 10 min at room temperature with 10 μl of either MccJ25 or t-MccJ25 dissolved in 10 % (v/v) methanol (final concentration 0.25–10 μM). Phage T5 was added to every well at time zero at an MOI (multiplicity of infection) of 2.5. Plates were then incubated under shaking in a Ceres 900 plate recorder at 37 °C, and bacterial growth and lysis were monitored over 120 min by measurement of the attenuance at 620 nm. A control for bacterial growth was performed in the presence of 0.25–10 μM microcin and in the absence of phage T5.

Inhibition of phage T5 adsorption on to *E. coli*

E. coli F in the exponential phase of growth were diluted to 2.5×10^8 c.f.u./ml in fresh LB medium and incubated further for 10 min at room temperature with MccJ25 or t-MccJ25 (0.1–10 μM), or with the microcin solvent only (50 % acetonitrile) as a control. Phage T5 was added to a final concentration of 2.5×10^9 p.f.u./ml (MOI = 10). After a 15 min incubation, phage adsorbed to the bacteria were eliminated by centrifugation (5 min, 10000 ***g***) and non-adsorbed phage were counted by determination of p.f.u. using a fresh suspension of *E. coli* F as an indicator strain.

Inhibition of phage T5 DNA ejection

FhuA (3 nM) was incubated for 10 min at room temperature with MccJ25 (50 nM–3.1 μM) or t-MccJ25 (3.1 μM) in assay buffer (150 mM NaCl, 1 % octyl glucoside, 25 mM Tris, pH 7.2) containing 4 μM fluorescent DNA intercalant YO-PRO-1 {quinolinium; 4-[(3-methyl-2(3*H*)-benzoxazolylidene)methyl]-1-[3-(trimethylammonio)propyl]; Molecular Probes}. Equal volumes (5 μl) of microcin solvent (50 % methanol) were present in every 800 μl assay. After equilibration of the FhuA/MccJ25 mixture in the spectrofluorimeter (10 min, 37 °C), phage T5 (2.5×10^9 p.f.u./ml) was added and DNA release was monitored over 10 min by fluorescence spectroscopy using a SLM8000 spectrofluorimeter ($\lambda_{excitation}$ 490 nm; $\lambda_{emission}$ 509 nm). The rate of fluorescence increase (V_f), which is directly proportional to the number of phage bound to FhuA in the linear part of the ejection curve, was calculated between 50 and 100 s after the addition of phage T5 [29]. The percentage of adsorbed phage in the presence of microcin (50 nM–3.1 μM) was calculated by comparing the measured V_f with a 100 % reference, determined in the absence of microcin. Data are representative of three independent experiments.

Characterization of the MccJ25–FhuA complex

Analytical size-exclusion chromatography

^{3}H-radiolabelled MccJ25 or t-MccJ25 (4 nmol) resuspended in 10 μl of FhuA buffer (150 mM NaCl, 1 % octyl glucoside, 25 mM Tris, pH 7.2) was incubated for 10 min in the presence of 250 μl of FhuA (4–16 nmol) or FhuA buffer only (control). The sample was then loaded on to a Superose 12 HR 10/30 column (Pharmacia) equilibrated with FhuA buffer. Separation was performed in the same buffer at room temperature at a flow rate of 0.25 ml/min. Absorbance was monitored at 226 nm. Radioactivity in every collected fraction was measured by using a Pharmacia Wallac 1410 liquid-scintillation counter.

For complex stability assays, a [^{3}H]MccJ25–FhuA complex was formed at a ligand/receptor ratio of 1:4 (mol/mol) and separated further from residual [^{3}H]MccJ25 as described above. The fractions containing the [^{3}H]MccJ25–FhuA complex were collected and concentrated by ultrafiltration (4500 ***g***, 45 min, 4 °C) on a MicroSep 10 K Omega spin column (Gelman Lab). The labelled complex was then re-injected on to the Superose 12 HR 10/30 column. Absorbance and radioactivity were monitored as described above.

All separations were performed on a Pharmacia AKTA Basic chromatography system.

Microcalorimetry

Buffers for samples (FhuA, MccJ25 and the MccJ25–FhuA complex) were exchanged by dialysis with 150 mM NaCl, 1 % octyl glucoside and 25 mM sodium phosphate, pH 7.3. Concentrations were adjusted according to the subsequent experiment, and samples were degassed thoroughly prior to recording thermograms. ITC (isothermal titration calorimetry) was performed at 25 °C on a VP-ITC calorimeter (MicroCal). A series of 28 injections of 500 μM MccJ25 (10 μl each) was performed at intervals of 1 min with a computer-controlled 300 μl microsyringe into a 26.5 μM FhuA solution (cell volume = 1.43 ml). A theoretical titration curve was fitted to the experimental data using ORIGIN® software (MicroCal). This software uses the relationship between the heat generated by each injection and ΔH (enthalpy change), K_a (association binding constant), n (number of binding sites per monomer), total protein concentration, and the concentrations of free and total ligand. DSC (differential scanning calorimetry) was carried out on a MicroCal model MC2 at a heating rate of 1 K/min between 20 and 90 °C. Each measurement was preceded by a baseline scan with the buffer. The heat capacity of the solvent was subtracted from that of the protein sample before analysis.

RESULTS

Antibacterial activity of MccJ25 and t-MccJ25

The antibacterial activity of MccJ25 was assayed against a series of Gram-positive and Gram-negative bacteria. Only two Enterobacteriaceae genera known to express the FhuA protein, namely *Escherichia* and *Salmonella*, were found to be susceptible to the microcin, with MIC values in the range $\leqslant$0.02–0.6 μM (Table 1A). The roles of the outer-membrane receptor FhuA as well as the inner-membrane complex TonB–ExbB–ExbD in the mechanism of action of MccJ25 were first investigated by assaying the antibacterial activity of a homogeneous MccJ25 preparation against wild-type and mutant isogenic strains bearing mutations in the *fhuA*, *tonB*, *exbB* and *exbD* genes. Our results showed that *fhuA*$^-$ *E. coli* C600, which is naturally tolerant to MccJ25 (MIC > 10 μM), became highly susceptible to the microcin (MIC $\leqslant$ 0.02 μM) upon transfection with the pHX405 plasmid encoding the *E. coli* FhuA protein (Table 1B). In addition, the loss of TonB or ExbB–ExbD conferred tolerance to *E. coli* W3110 (MIC and MBC > 10 μM), whereas the wild-type strain was susceptible to MccJ25, with MIC and MBC values of 0.6 and 10 μM respectively (Table 1B). Therefore both FhuA and the TonB–ExbB–ExbD complex are required for the antibacterial activity of Mcc25 against *E. coli*.

In order to determine whether the Val^{11}–Pro^{16} β-hairpin region of MccJ25, which is disrupted upon cleavage by thermolysin of the Phe^{10}–Val^{11} bond [4] (Figure 1), is required for the antibacterial activity of the peptide, the MIC and MBC values of MccJ25 were compared with those of its thermolysin-cleaved variant, t-MccJ25. Upon cleavage by thermolysin, MIC values increased at least 15-fold and MBC values shifted over 10 μM, compared with values of 0.04–10 μM respectively for uncleaved MccJ25, for action against the microcin-susceptible bacteria *S. enterica* Paratyphi SL369, *S. enterica* Enteritidis and *E. coli* W3110 (Table 1A). Altogether, these data are indicative of a significant loss of activity of the microcin upon cleavage by thermolysin.

These results prompted us to investigate the role of the thermolysin-targeted region of MccJ25 in the process of recognition by the FhuA receptor. Subsequent *in vivo* assays were consequently

Table 1 Antibacterial activity of MccJ25 and t-Mcc25

(**A**) Spectrum of antibacterial activity; (**B**) antibacterial activity of MccJ25 against wild-type and mutant strains of *E. coli*. MIC values are expressed as the lowest microcin concentration that caused 100 % inhibition in liquid growth-inhibition assays. MBC values are expressed as the lowest microcin concentration for which no activity (c.f.u.) was counted on agar plates. NA, not active in the range 0.02–10 μM.

(A)

	MccJ25 (μM)		t-MccJ25 (μM)	
Bacterium	MIC	MBC	MIC	MBC
Gram-negative bacteria				
Escherichia coli W3110	0.60	10	NA	NA
Enterobacter cloacae	NA	NA	NA	NA
Erwinia carotovora	NA	NA	NA	NA
Klebsiella pneumoniae	NA	NA	NA	NA
Pantoea agglomerans K4	NA	NA	NA	NA
Pseudomonas aeruginosa	NA	NA	NA	NA
Salmonella enterica Enteritidis	0.04	5	1.20	NA
Salmonella enterica Paratyphi SL369	$\leqslant$ 0.02	0.04	0.30	NA
Salmonella enterica Typhimurium LT2	NA	NA	NA	NA
Vibrio harveyi	NA	NA	NA	NA
Gram-positive bacteria				
Aerococcus viridans	NA	NA	NA	NA
Bacillus megaterium	NA	NA	NA	NA
Staphylococcus aureus	NA	NA	NA	NA

(B)

	MccJ25 (μM)	
Strain	MIC	MBC
W3110	0.60	10
W3110 KP1344 (*tonB*$^-$)	NA	NA
W3110-6 (*exbBD*$^-$)	NA	NA
C600 (*fhuA*$^-$)	NA	NA
C600 (*fhuA*$^-$) pHX405	$\leqslant$ 0.02	1.20

designed to characterize MccJ25 recognition without considering its intracellular mechanism of action.

Inhibition of the bacterial lysis by phage T5

Infection of *E. coli* by phage T5 is initiated by the irreversible binding of the phage to FhuA. We therefore investigated whether MccJ25 interferes with phage T5 infection. The phage-induced lysis of *E. coli* F (a wild-type strain for FhuA and TonB–ExbB–ExbD) was measured in the presence of MccJ25. Control experiments showed that MccJ25 or t-MccJ25 alone had little or no effect on *E. coli* F growth at concentrations ranging from 0.5 to 10 μM (results not shown). In the absence of MccJ25, bacterial lysis occurred 50 min after phage T5 addition (Figure 2A). However, addition of MccJ25 prior to phage incubation resulted in a dose-dependent inhibition of lysis. Bacterial growth started to be restored by 0.5 μM MccJ25, and was similar to that observed in the absence of phage T5 when 10 μM MccJ25 was added (Figure 2A). Therefore 10 μM MccJ25 fully inhibited the phage-induced lysis of *E. coli* F. In contrast, bacterial growth could not be restored upon addition of t-MccJ25 over the same range of concentrations (0.5–10 μM) (Figure 2B).

Inhibition of phage T5 adsorption to *E. coli* F

In order to determine whether the MccJ25-mediated inhibition of phage infection was due to inhibition of the interaction between the phage and its receptor FhuA, or to a later event, we measured phage adsorption to *E. coli* F in the presence of MccJ25 or

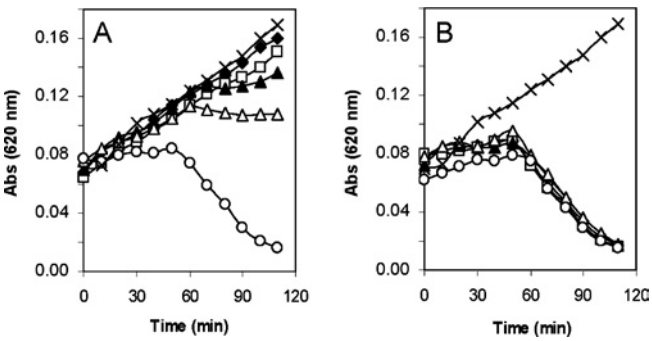

Figure 2 Inhibitory effects of Mcc25 and t-MccJ25 on infection by phage T5

E. coli F was incubated with MccJ25 (**A**) or t-MccJ25 (**B**) at concentrations of 0.5 μM (△), 1 μM (▲), 5 μM (□) and 10 μM (◆), or with solvent only (○). After addition of phage T5, the culture turbidity (Abs) was monitored over 120 min at 620 nm. A control was performed in the absence of phage T5 (×). Data are representative of four independent experiments.

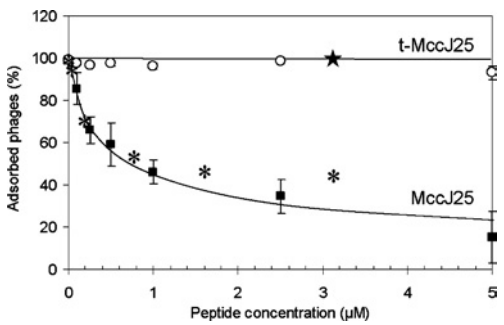

Figure 3 Inhibition of phage T5 adsorption

Phage adsorption was first measured *in vivo* by incubating *E. coli* W3110 for 10 min with 0.1–10 μM MccJ25 (■) or t-MccJ25 (○) before addition of phage T5. The amount of adsorbed phage was determined after a 15 min incubation with phage T5 at MOI = 10. Results are expressed as means ± S.E.M. for three independent experiments. *In vitro*, phage adsorption to FhuA was evaluated by measuring the microcin-induced inhibition of DNA ejection. FhuA (3 nM) was incubated for 10 min with 0.1, 0.2, 0.8, 1.6 or 3.1 μM MccJ25 (∗) or solvent only in the presence of the fluorescent probe YO-PRO-1. The reaction was initiated by phage T5 addition. The inhibitory activity of 3.1 μM t-MccJ25 (black star) was compared with that of MccJ25 at the same concentration. The fluorescence signal indicative of phage DNA release was measured over 10 min ($\lambda_{excitation}$ 490 nm; $\lambda_{emission}$ 509 nm). The rate of fluorescence increase (V_f), which is directly proportional to the number of phage bound to FhuA, was measured in order to calculate the percentage of adsorbed phage. Data are representative of three independent experiments.

t-MccJ25. Upon addition of increasing concentrations of MccJ25 to the bacteria prior to phage T5, the number of adsorbed phage decreased from 80 % at 0.1 μM MccJ25 to 15 % at 5 μM MccJ25 (Figure 3). Conversely, t-MccJ25 did not inhibit phage adhesion over the same range of concentrations (Figure 3).

In vitro inhibition of DNA release induced by binding of phage T5 to FhuA

In order to assess whether the inhibition of phage adhesion to *E. coli* was due solely to binding of MccJ25 to FhuA, the FhuA–phage T5 interaction was monitored *in vitro* after pre-incubation of FhuA with MccJ25. Previous experiments [29] have shown that phage T5 ejects its DNA upon binding to purified FhuA, and DNA release can be measured using the fluorescent DNA intercalant YO-PRO-1. Addition of increasing concentrations of MccJ25 to FhuA prior to incubation with phage T5 resulted in a concomitant decrease in YO-PRO-1 fluorescence (results not shown). From the

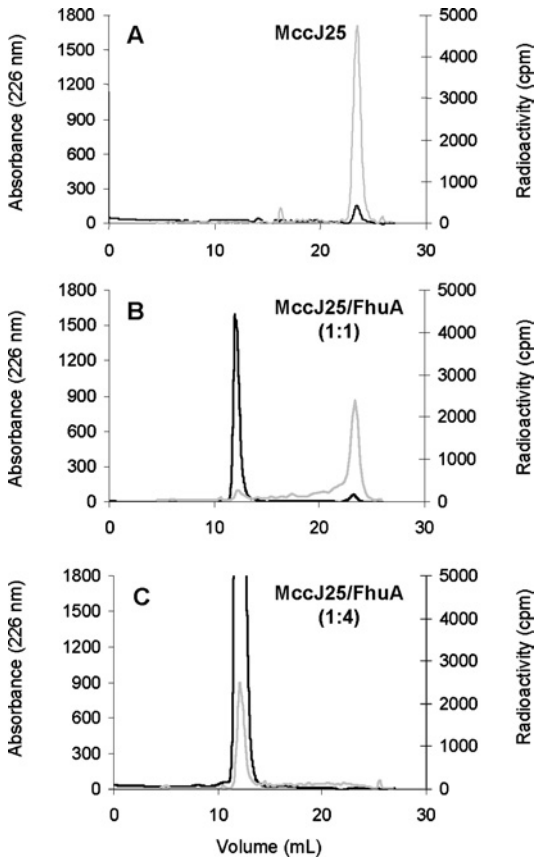

Figure 4 MccJ25–FhuA interaction *in vitro*

^{3}H-labelled MccJ25 (4 nmol) was incubated for 10 min in the presence of 4 nmol (**B**) or 16 nmol (**C**) of FhuA. In a control experiment (**A**), incubation was performed in FhuA buffer only. Samples were analysed by gel-permeation chromatography on a Superose 12 HR 10/30 column. Absorbance was monitored at 226 nm (black line). Radioactivity was measured in every collected fraction by liquid scintillation counting (grey line).

V_f measurements, we calculated that the proportion of adsorbed phage decreased from 100 to 45 % when increasing the MccJ25 concentration from 0.1 to 3.2 μM (Figure 3). These values are in good agreement with the *in vivo* inhibition data (Figure 3). Finally, as shown *in vivo*, addition of t-MccJ25 had no detectable effect on T5 DNA ejection (Figure 3). Taken together, these data suggest that MccJ25 competes with phage T5 for binding to FhuA both *in vivo* and *in vitro*.

In vitro MccJ25–FhuA complex formation

The putative binding of MccJ25 to FhuA was investigated by gel filtration. Purified FhuA (79 kDa) and MccJ25 (2 kDa) eluted as well separated peaks from a Superose 12 column, with retention volumes of 12.0 ml and 23.2 ml respectively (Figures 4A and 4B). Owing to the low molecular mass of MccJ25 compared with that of FhuA, isolated FhuA could not be separated from a putative MccJ25–FhuA complex by gel filtration. Therefore ^{3}H-labelled MccJ25 was used instead of unlabelled MccJ25, and the radioactivity associated with the microcin was measured in the collected fractions. [^{3}H]MccJ25 and FhuA were mixed at molar ratios ranging from 1:1 to 1:4 and incubated prior to gel filtration analysis. The radioactivity initially associated with the [^{3}H]-MccJ25 peak shifted to the FhuA fraction, in which it was fully recovered at a 1:4 [^{3}H]MccJ25/FhuA molar ratio (Figures 4B and 4C). This suggested that [^{3}H]MccJ25 and FhuA formed a complex, and that all of the microcin was associated with FhuA when the receptor was in excess. The strength of the interaction was evaluated by reloading the [^{3}H]MccJ25–FhuA fractions on to the same column after concentration by ultrafiltration. The radioactivity again eluted as a single peak corresponding to the FhuA elution volume, without any significant release of radioactivity at the microcin elution volume (results not shown).

In order to determine whether the lack of activity of t-MccJ25 in the previous assays (antibacterial activity and inhibition of FhuA-dependent functions) could be due to a lack of affinity of the thermolysin-cleaved microcin for the FhuA receptor, we performed the same complex formation assays by incubating t-MccJ25 with FhuA in a 1:4 molar ratio. Unlike MccJ25, t-MccJ25 was unable to bind to FhuA, as indicated by equal absorbance of the t-MccJ25 peak in the presence or in the absence of FhuA (results not shown).

Affinity constant for binding of MccJ25 to FhuA

The MccJ25–FhuA interaction was characterized further using ITC, a powerful technique for determining the affinity, stoichiometry and thermodynamic parameters of receptor–ligand interactions. The titration of FhuA with MccJ25 (described in the Experimental section) was exothermic, with $\Delta H = 14$ kJ/mol (Figure 5A). The best fit to the experimental data was obtained for a binding curve corresponding to a one-class binding site model and a stoichiometry of 1.9, consistent with the binding of two microcins per FhuA (Figure 5A). The threshold at which no further heat was generated upon microcin addition was reached at MccJ25/FhuA molar ratios above 3:1. In agreement with the size-exclusion chromatography data, this indicates that a 3–4-fold molar excess of either the ligand or the receptor shifts the reaction towards complex formation. From the ITC data analysis, this affinity was characterized by a K_d value of 1.2 μM.

To analyse further the effect of binding of MccJ25 to FhuA, thermal denaturation of the complex was compared by DSC with that of FhuA alone. FhuA displays two well resolved thermal transitions, corresponding to the unfolding of the loops and plug, and to the unfolding of the β-barrel [20,28]. Under our experimental conditions, these were observed at 63 and 70 °C respectively (Figure 5B). Interestingly, DSC of the MccJ25–FhuA complex formed under conditions of complete saturation by MccJ25 (80 μM MccJ25 and 20 μM FhuA) showed a higher ΔH for the denaturation of the first domain, which corresponds to the loops and plug (706 kJ/mol, compared with 356 kJ/mol for FhuA alone, as calculated from Figure 5B). The unfolding of the second domain remained almost unchanged (Figure 5B). A fall in ΔCp (excess calorimatric capacity) was observed with both the FhuA and MccJ25–FhuA denaturation curves at 72–73 °C due to heat-induced aggregation. The lack of a signal for unbound MccJ25 is most probably related to its remarkable temperature stability [5]. This was confirmed in a control experiment in which MccJ25 alone gave no enthalpy signal (results not shown).

DISCUSSION

The present study was performed using *in vivo* and *in vitro* quantitative approaches to demonstrate the role of FhuA in the antibacterial activity of MccJ25 and its recognition at the outer membrane of target bacteria.

MccJ25 antimicrobial activity was found to be limited to a few species of Enterobacteriaceae, which were affected by the microcin in the nanomolar range. Unlike most antimicrobial peptides that display low specificity and MIC values in the range 0.1–20 μM associated with a membrane-permeabilizing activity

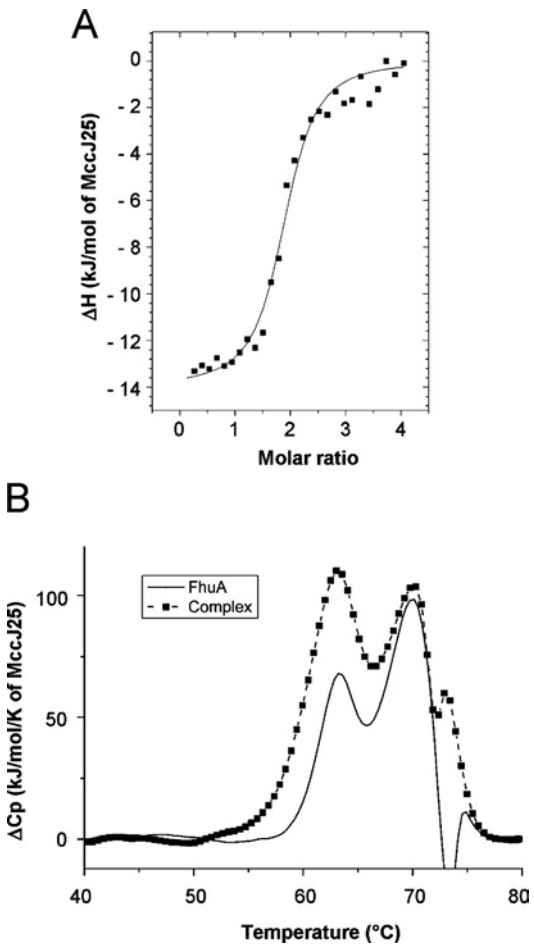

Figure 5 Microcalorimetry analysis

(**A**) Microcalorimetric titration isotherm for the binding of MccJ25 to FhuA. Data were obtained at 25 °C using an automated sequence of 28 injections of 500 μM MccJ25 from a 300 μl syringe into a reaction cell containing 26.5 μM FhuA. The volume of each injection was 10 μl, and injections were made at 1 min intervals. Raw data were treated with ORIGIN® software and the values are plotted against molar ratio. Each point corresponds to the heat generated by the reaction upon each injection. The curve fit to the data (solid line) obtained by the ORIGIN® software yields values for K_d and stoichiometry (see the Experimental section). (**B**) DSC endotherm of the MccJ25–FhuA complex. Baseline-corrected DSC thermograms of FhuA alone (13 μM) (solid line) and the MccJ25–FhuA complex formed by complete saturation of FhuA with MccJ25 (broken line) were recorded in the same buffer as for ITC experiments with a heating rate of 1 K/min.

[30–32], the narrow spectrum of activity and the high potency of MccJ25 are reminiscent of a receptor-mediated mechanism of action. Interestingly, in our antibacterial assays, only four bacterial species belonging to the *Escherichia* and *Salmonella* genera, known to express FhuA, were MccJ25-susceptible. In agreement with previous studies [11], our results with bacterial mutants confirmed that FhuA expression is required for susceptibilty to MccJ25. Indeed, the MccJ25-resistant *E. coli* C600 (*fhuA*$^-$) became highly susceptible (MIC $\leqslant$ 0.02 μM) upon transfection with the FhuA-encoding plasmid pHX405. In addition, we showed that mutations in genes encoding proteins of the TonB–ExbB–ExbD complex also resulted in a complete loss of susceptibility to MccJ25, as revealed by a shift in MIC from 0.6 μM against the wild-type *E. coli* W3110 strain to above 10 μM against the *tonB*$^-$ and *exbBD*$^-$ isogenic strains. This result is in agreement with the isolation of *tonB* mutants of *E. coli* resistant to MccJ25 [10]. The double dependence on FhuA and the TonB complex supports the hypothesis that MccJ25 first binds to the receptor FhuA and then requires the TonB–ExbB–ExbD complex for its uptake into the target bacterium.

Whereas in earlier studies various stable ligand–FhuA complexes could be isolated, providing both thermodynamic and physicochemical parameters of the interaction and structural characterization of the complex [15], no evidence of MccJ25–FhuA complex formation had been reported. The availability of highly pure solutions of MccJ25 and FhuA allowed us to perform both *in vivo* and *in vitro* assays, which permitted us to characterize the interaction between the microcin and its putative receptor independent of any other step of the antibacterial mechanism, such as the inhibition of the host RNA polymerase [6,7] that occurs after the recognition/binding and transport steps. MccJ25 was used to inhibit the well described recognition of phage T5 by FhuA. We demonstrated that, *in vivo*, MccJ25 inhibited phage infection and subsequent bacterial lysis in a dose-dependent manner, and that full inhibition was achieved with 10 μM MccJ25. In addition, pre-incubation of *E. coli* with increasing MccJ25 concentrations (0–10 μM) resulted in decreasing amounts of adsorbed phage. It is therefore very likely that blocking of phage infection results from inhibition of the irreversible binding of phage T5 to FhuA. Interestingly, similar inhibition of phage T5 adsorption was observed *in vitro*. Indeed, MccJ25 was able to inhibit the release of phage T5 DNA induced by the irreversible binding of phage T5 to FhuA that had been previously solubilized and purified in the presence of detergent, and thus deprived of any other bacterial components. Remarkably, *in vitro* and *in vivo* data matched perfectly, as indicated by very similar inhibition values with increasing MccJ25 concentration. Therefore, *in vitro* data can be considered to be reliable for the description of the MccJ25–FhuA interaction *in vivo*. Altogether, these results demonstrate that MccJ25-induced inhibition of phage adhesion results from direct interaction of MccJ25 with the FhuA receptor.

Evidence for actual binding of MccJ25 to FhuA was first obtained by size-exclusion chromatography. In the presence of excess FhuA, ^{3}H-labelled MccJ25 eluted in the FhuA fraction (79 kDa) instead of in the original MccJ25 fraction (2 kDa). The complex was found to be stable, since no detectable MccJ25 release was observed upon re-injection of the complex on to the column. ITC confirmed this complex formation, and gave a MccJ25–FhuA dissociation constant of 1.2 μM. Similar affinities were measured for interactions between colicins (larger-size bacterial toxins) and their outer-membrane receptors. Thus, *in vitro*, ITC gave a K_d value of 2 μM for binding of colicin N to OmpF [33], while *in vivo*, colicins B and D were shown to bind to the enterobactin receptor FepA with K_d values of 0.185 and 0.560 μM respectively [34]. In addition, ITC data indicated that, *in vitro*, MccJ25 binds to one single class of sites, with a stoichiometry consistent with two ligands per receptor ($n = 1.9$). By comparing the thermal denaturation profile of the MccJ25–FhuA complex with that of FhuA, which presents two transitions as characterized previously [20,28], we showed that MccJ25 binding affected only the external loops and plug (first domain) of FhuA, and not the β-barrel (second domain). Indeed, unfolding of the first domain required a much higher enthalpy when MccJ25 was associated with FhuA, indicating that stabilization of the first domain results from binding of MccJ25 to FhuA.

Since MccJ25 is not likely to bind to the plug buried within the β-barrel, our results strongly suggest that binding occurs through the external loops accessible to the various ligands of FhuA. This hypothesis is in agreement with recent findings on the role of these external loops in the transport and receptor functions of FhuA: analysis of the phenotype of *E. coli* mutants expressing different FhuA proteins lacking one of the 11 external loops showed that

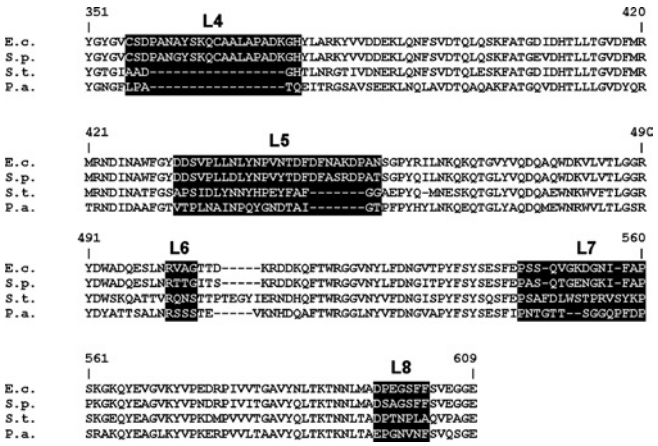

Figure 6 Partial alignment of FhuA amino acid sequences from MccJ25-susceptible (E.c., S.p.) and MccJ25-tolerant (S.t., P.a.) strains

Alignment was performed using the Multalign software [39]. Extracellular loops L4–L8 of the *E. coli* FhuA protein [12] are in black boxes, together with the corresponding sequence in other Enterobacteriaceae. Abbreviations and sources for the sequences are: E.c, *E. coli* K12 W3110 (Swiss-Prot; accession no. P0671); S.p., *S. enterica* Paratyphi SL369 (TrEMBL; accession no O86903); S.t., *S. enterica* Typhimurium LT2 (TrEMBL; accession no O86925); P.a., *P. agglomerans* K4 (TrEMBL; accession no O86924).

loops L5, L7, L8 and L11 are essential for MccJ25 activity, and that loop L8 can be considered as the major and maybe the single binding site for phage T5 [16]. Together with this finding, the ability of MccJ25 to prevent the FhuA–phage T5 interaction in our *in vivo* and *in vitro* assays suggests that MccJ25 and phage T5 bind to the same loop L8 on the FhuA receptor. A major role for the external loops in MccJ25 binding is also supported by a comparative analysis of the sequences of the FhuA proteins originating from both MccJ25-tolerant (*S. enterica* Typhimurium LT2 and *P. agglomerans*) and MccJ25-susceptible (*E. coli* W3110 and *S. enterica* Paratyphi SL369) bacteria (Figure 6). The overall sequence of FhuA is highly conserved among both susceptible and tolerant strains [35], with the exception of the external loops L4–L8. Indeed, the FhuA sequences from tolerant strains show two conserved deletions of 17 and seven amino acids within loops L4 and L5 respectively, as well as significant divergence within loops L7 and L8, as compared with the FhuA sequences from susceptible strains (Figure 6). Altogether, these results suggest that, by modifying the conformation of FhuA loops L5, L7 and/or L8, bacteria could prevent MccJ25 binding and therefore gain resistance to the microcin.

In all of the experiments discussed above, MccJ25 was compared with its thermolysin-cleaved variant t-MccJ25. This latter peptide failed to inhibit FhuA binding properties and did not bind to FhuA under the conditions used for the native peptide. This indicates that binding of MccJ25 to FhuA is specific and does not result artifactually from biophysical characteristics such as hydrophobicity.

The weak antibacterial activity of t-MccJ25 is indicative of a critical role for the Val^{11}–Pro^{16} β-hairpin in the antibacterial activity of MccJ25. Indeed, the three-dimensional structure of the entire region is lost upon cleavage by thermolysin [4]. Recent studies have shown that this region is not required for inhibition of bacterial RNA polymerase [36,37] but did not investigate its potential role in MccJ25 recognition. We show here that the MccJ25–FhuA molecular interaction cannot be observed when the thermolysin-cleaved variant t-MccJ25 is used, indicating that cleavage of MccJ25 induces a major loss of affinity for the FhuA receptor. Moreover, unlike with MccJ25, no inhibitory effect of t-MccJ25 was observed on phage T5 adhesion, DNA ejection and subsequent bacterial lysis. In summary, the present study provides the first evidence for a critical role for the Val^{11}–Pro^{16} region for MccJ25 recognition at the bacterial membrane. It is concluded that the MccJ25 threaded cyclic backbone, the structure of which is retained upon cleavage by thermolysin [4], should play a major role in the RNA polymerase inhibitory activity of the microcin.

This investigation was supported by the Centre National de la Recherche Scientifique (CNRS) and the Muséum National d'Histoire Naturelle (MNHN), France. We are grateful to Magali Nicaise, Chantal Herbeuval, Alain Blond, Gérard Gastine and Julie de Azevedo for invaluable technical assistance, as well as Geneviève Auger for amino acid composition analysis. We are indebted to Volkmar Braun (University of Tübingen, Germany), Felipe Moreno (Hospital Ramón y Cajal, Madrid, Spain) and Alain Reynaud (Hospital of Nantes, France) for generously providing bacterial strains.

REFERENCES

1 Salomón, R. A. and Farías, R. N. (1992) Microcin 25, a novel antimicrobial peptide produced by *Escherichia coli*. J. Bacteriol. **174**, 7428–7435
2 Blond, A., Péduzzi, J., Goulard, C., Chiuchiolo, M. J., Barthélémy, M., Prigent, Y., Salomón, R. A., Farías, R. N., Moreno, F. and Rebuffat, S. (1999) The cyclic structure of microcin J25, a 21-residue peptide antibiotic from *Escherichia coli*. Eur. J. Biochem. **259**, 747–755
3 Rosengren, K. J., Clark, R. J., Daly, N. L., Goransson, U., Jones, A. and Craik, D. J. (2003) Microcin J25 has a threaded sidechain-to-backbone ring structure and not a head-to-tail cyclized backbone. J. Am. Chem. Soc. **125**, 12464–12474
4 Rosengren, K. J., Blond, A., Afonso, C., Tabet, J. C., Rebuffat, S. and Craik, D. J. (2004) Structure of thermolysin cleaved microcin J25: extreme stability of a two-chain antimicrobial peptide devoid of covalent links. Biochemistry **43**, 4696–4702
5 Blond, A., Cheminant, M., Destoumieux-Garzón, D., Ségalas-Milazzo, I., Péduzzi, J., Goulard, C. and Rebuffat, S. (2002) Thermolysin-linearized microcin J25 retains the structured core of the native macrocyclic peptide and displays antimicrobial activity. Eur. J. Biochem. **269**, 6212–6222
6 Yuzenkova, J., Delgado, M., Nechaev, S., Savalia, D., Epshtein, V., Artsimovitch, I., Mooney, R. A., Landick, R., Farías, R. N., Salomón, R. and Severinov, K. (2002) Mutations of bacterial RNA polymerase leading to resistance to microcin J25. J. Biol. Chem. **277**, 50867–50875
7 Delgado, M. A., Rintoul, M. R., Farías, R. N. and Salomón, R. A. (2001) *Escherichia coli* RNA polymerase is the target of the cyclopeptide antibiotic microcin J25. J. Bacteriol. **183**, 4543–4550
8 Adelman, K., Yuzenkova, J., La Porta, A., Zenkin, N., Lee, J., Lis, J. T., Borukhov, S., Wang, M. D. and Severinov, K. (2004) Molecular mechanism of transcription inhibition by peptide antibiotic microcin J25. Mol. Cell **14**, 753–762
9 Mukhopadhyay, J., Sineva, E., Knight, J., Levy, R. M. and Ebright, R. H. (2004) Antibacterial peptide microcin J25 inhibits transcription by binding within and obstructing the RNA polymerase secondary channel. Mol. Cell **14**, 739–751
10 Salomón, R. A. and Farías, R. N. (1995) The peptide antibiotic microcin 25 is imported through the TonB pathway and the SbmA protein. J. Bacteriol. **177**, 3323–3325
11 Salomón, R. A. and Farías, R. N. (1993) The FhuA protein is involved in microcin 25 uptake. J. Bacteriol. **175**, 7741–7742
12 Braun, V. and Braun, M. (2002) Active transport of iron and siderophore antibiotics. Curr. Opin. Microbiol. **5**, 194–201
13 Coulton, J. W., Mason, P. and DuBow, M. S. (1983) Molecular cloning of the ferrichrome-iron receptor of *Escherichia coli* K-12. J. Bacteriol. **156**, 1315–1321
14 Hantke, K. and Braun, V. (1978) Functional interaction of the TonA/TonB receptor system in *Escherichia coli*. J. Bacteriol. **135**, 190–197
15 Locher, K. P., Rees, B., Koebnik, R., Mitschler, A., Moulinier, L., Rosenbusch, J. P. and Moras, D. (1998) Transmembrane signaling across the ligand-gated FhuA receptor: crystal structures of free and ferrichrome-bound states reveal allosteric changes. Cell **95**, 771–778
16 Endriss, F. and Braun, V. (2004) Loop deletions indicate regions important for FhuA transport and receptor functions in *Escherichia coli*. J. Bacteriol. **186**, 4818–4823
17 Killmann, H., Braun, M., Herrmann, C. and Braun, V. (2001) FhuA barrel-cork hybrids are active transporters and receptors. J. Bacteriol. **183**, 3476–3487
18 Vincent, P. A., Delgado, M. A., Farías, R. N. and Salomón, R. A. (2004) Inhibition of *Salmonella enterica* serovars by microcin J25. FEMS Microbiol. Lett. **236**, 103–107
19 Solbiati, J. O., Ciaccio, M., Farías, R. N. and Salomón, R. A. (1996) Genetic analysis of plasmid determinants for microcin J25 production and immunity. J. Bacteriol. **178**, 3661–3663

20 Bonhivers, M., Desmadril, M., Moeck, G. S., Boulanger, P., Colomer-Pallas, A. and Letellier, L. (2001) Stability studies of FhuA, a two-domain outer membrane protein from *Escherichia coli*. Biochemistry **40**, 2606–2613
21 Destoumieux-Garzón, D., Thomas, X., Santamaria, M., Goulard, C., Barthélémy, M., Boscher, B., Bessin, Y., Molle, G., Pons, A. M., Letellier, L. et al. (2003) Microcin E492 antibacterial activity: evidence for a TonB-dependent inner membrane permeabilization on *Escherichia coli*. Mol. Microbiol. **49**, 1031–1041
22 Thomas, X., Destoumieux-Garzón, D., Péduzzi, J., Afonso, C., Blond, A., Birlirakis, N., Goulard, C., Dubost, L., Thai, R., Tabet, J. C. and Rebuffat, S. (2004) Siderophore peptide, a new type of post-translationally modified antibacterial peptide with potent activity. J. Biol. Chem. **279**, 28233–28242
23 Graham, A. C. and Stocker, B. A. (1977) Genetics of sensitivity of *Salmonella* species to colicin M and bacteriophages T5, T1, and ES18. J. Bacteriol. **130**, 1214–1223
24 Berner, I., Konetschny-Rapp, S., Jung, G. and Winkelmann, G. (1988) Characterization of ferrioxamine E as the principal siderophore of *Erwinia herbicola* (*Enterobacter agglomerans*). Biol. Met. **1**, 51–56
25 Hill, C. W. and Harnish, B. W. (1981) Inversions between ribosomal RNA genes of *Escherichia coli*. Proc. Natl. Acad. Sci. U.S.A. **78**, 7069–7072
26 Heller, K. and Braun, V. (1979) Accelerated adsorption of bacteriophage T5 to *Escherichia coli* F, resulting from reversible tail fiber-lipopolysaccharide binding. J. Bacteriol. **139**, 32–38
27 Bonhivers, M., Ghazi, A., Boulanger, P. and Letellier, L. (1996) FhuA, a transporter of the *Escherichia coli* outer membrane, is converted into a channel upon binding of bacteriophage T5. EMBO J. **15**, 1850–1856
28 Plançon, L., Janmot, C., le Maire, M., Desmadril, M., Bonhivers, M., Letellier, L. and Boulanger, P. (2002) Characterization of a high-affinity complex between the bacterial outer membrane protein FhuA and the phage T5 protein pb5. J. Mol. Biol. **318**, 557–569
29 Boulanger, P., le Maire, M., Bonhivers, M., Dubois, S., Desmadril, M. and Letellier, L. (1996) Purification and structural and functional characterization of FhuA, a transporter of the *Escherichia coli* outer membrane. Biochemistry **35**, 14216–14224
30 Hancock, R. E. and Chapple, D. S. (1999) Peptide antibiotics. Antimicrob. Agents Chemother. **43**, 1317–1323
31 Ganz, T. and Lehrer, R. I. (1995) Defensins. Pharmacol. Ther. **66**, 191–205
32 Bulet, P., Hétru, C., Dimarcq, J. L. and Hoffmann, D. (1999) Antimicrobial peptides in insects; structure and function. Dev. Comp. Immunol. **23**, 329–344
33 Evans, L. J., Cooper, A. and Lakey, J. H. (1996) Direct measurement of the association of a protein with a family of membrane receptors. J. Mol. Biol. **255**, 559–563
34 Payne, M. A., Igo, J. D., Cao, Z., Foster, S. B., Newton, S. M. and Klebba, P. E. (1997) Biphasic binding kinetics between FepA and its ligands. J. Biol. Chem. **272**, 21950–21955
35 Killmann, H., Herrmann, C., Wolff, H. and Braun, V. (1998) Identification of a new site for ferrichrome transport by comparison of the FhuA proteins of *Escherichia coli*, *Salmonella paratyphi* B, *Salmonella typhimurium*, and *Pantoea agglomerans*. J. Bacteriol. **180**, 3845–3852
36 Semenova, E., Yuzenkova, J., Péduzzi, J., Rebuffat, S. and Severinov, K. (2005) Structure-activity analysis of microcin J25: distinct parts of the threaded lasso molecule are responsible for interaction with bacterial RNA polymerase. J. Bacteriol. **187**, 3859–3863
37 Bellomio, A., Vincent, P. A., de Arcuri, B. F., Salomón, R. A., Morero, R. D. and Farías, R. N. (2004) The microcin J25 beta-hairpin region is important for antibiotic uptake but not for RNA polymerase and respiration inhibition. Biochem. Biophys. Res. Commun. **325**, 1454–1458
38 Koradi, R., Billeter, M. and Wüthrich, K. (1996) MOLMOL: a program for display and analysis of macromolecular structures. J. Mol. Graphics **14**, 51–55
39 Corpet, F. (1988) Multiple sequence alignment with hierarchical clustering. Nucleic Acids Res. **16**, 10881–10890

Received 20 December 2004/7 April 2004; accepted 29 April 2005
Published as BJ Immediate Publication 29 April 2005, DOI 10.1042/BJ20042107